Recombinant nematode anticoagulant protein c2 inhibits cell invasion by decreasing uPA expression in NSCLC cells

YU TONG[1,2*], JUN YUE[4*], MENG MAO[1,2], QINGQING LIU[1,2], JING ZHOU[5] and JIYUN YANG[3]

[1]Laboratory of Early Developmental Injuries, West China Institute of Woman and Children's Health, and Department of Pediatrics, West China Second University Hospital, Sichuan University; [2]Key Laboratory of Obstetric and Gynecologic and Pediatric Diseases and Birth Defects of the Ministry of Education; [3]Center for Human Molecular Biology and Genetics, The Key Laboratory for Human Disease Gene Study of Sichuan Province, Sichuan Academy of Medical Sciences and Sichuan Provincial People's Hospital; [4]Department of Gynecology and Obstetrics, Sichuan Academy of Medical Sciences and Sichuan Provincial People's Hospital; [5]Department of Laboratory Medicine, West China Hospital, Sichuan University, Chengdu, Sichuan 610041, P.R. China

Received October 24, 2014; Accepted January 23, 2015

DOI: 10.3892/or.2015.3795

Abstract. Nematode anticoagulant protein c2 (NAPc2) is an 85-residue polypeptide originally isolated from the hematophagous hookworm, *Ancylostoma caninum*. Several studies have shown that rNAPc2 inhibits the growth of primary and metastatic tumors in mice independently of its ability to initiate coagulation. We obtained bioactive recombinant rNAPc2 by splicing of the rNAPc2-intein-CBD fusion proteins expressed in *E. coli* ER2566. In the *in vitro* assay, rNAPc2 obviously inhibited the invasive ability of non-small cell lung cancer (NSCLC) cells in a dose-dependent manner. Furthermore, rNAPc2 suppressed tumor growth *in vivo* by daily intraperitoneal injection of rNAPc2 in an NSCLC cell xenograft model of nude mice. Respectively, rNAPc2 downregulated the production of urokinase plasminogen activator (uPA) ($P<0.05$) and suppressed nuclear factor-κB (NF-κB) activity. We also identified that inhibition of NF-κB activity impaired cell invasion and reduced the uPA production in NSCLC cells. Meanwhile, NF-κB was found to directly bind to the uPA promoter *in vitro*. These results demonstrated that rNAPc2 inhibits cell invasion at least in part through the downregulation of the NF-κB-dependent metastasis-related gene expression in NSCLC. Our results also suggest that uPA, a known metastasis-promoting gene, is indirectly regulated by rNAPc2 through NF-κB activation. These results indicate that rNAPc2 may be a potent agent for the prevention of NSCLC progression.

Correspondence to: Dr Jiyun Yang, Center for Human Molecular Biology and Genetics, The Key Laboratory for Human Disease Gene Study of Sichuan Province, Sichuan Academy of Medical Sciences and Sichuan Provincial People's Hospital, The Western First Round Road 32, Section 2, Chengdu, Sichuan 610072, P.R. China
E-mail: yangjiyun@yeah.net

*Contributed equally

Key words: nematode anticoagulant protein c2, cell invasion, urokinase plasminogen activator, nuclear factor-κB, non-small cell lung cancer

Introduction

Lung cancer continues to be the leading cause of cancer-related mortality worldwide. Non-small cell lung cancer (NSCLC) accounts for ~85% of all the cases of lung cancer (1). Lung cancer is a highly metastatic disease, and the mortality of this type of cancer is strongly associated with its high tendency to metastasize to specific organs. Most patients present locally advanced or metastatic disease at the time of diagnosis. Chemotherapy remains the mainstay of treatment for patients with metastatic NSCLC. The median survival time for advanced NSCLC patients remains poor. Therefore, it is necessary to develop new drugs to improve the survival rate of lung cancer patients (2,3).

Nematode anticoagulant protein c2 (NAPc2) is an 85-residue polypeptide originally isolated from the hematophagous hookworm, *Ancylostoma caninum* (3,4). NAPc2 is a potent inhibitor of factor X (FX) activation by the extrinsic Xase complex composed of VIIa and tissue factor (5-7). It targets a specific site in the primary stages of the coagulation pathway; it binds to FX or activated factor X (FXa) prior to the formation of an inhibitory complex with activated factor VII/tissue factor (FVIIa/TF). This inhibits coagulation and decreases the formation of fibrin. The high affinity interaction between NAPc2 and FX is decisive for its pharmacokinetics. NAPc2 is potentially an attractive agent, for its elimination half-life was found to be longer than 50 h following subcutaneous and intravenous administration in healthy male volunteers (6). Recombinant rNAPc2 has been shown to be very effective in reducing the incidence of deep venous thrombosis without hemostatic compromise when administered prophylactically in patients (8). Furthermore, rNAPc2 inhibits the growth of primary and metastatic tumors

in mice independently of its ability to initiate coagulation (9). rNAPc2 can inhibit colorectal tumorigenesis, progression and metastasis in mice through a TF-dependent mechanism, indicating that rNAPc2 is a potent anticancer agent when used in combination with chemotherapy or anti-angiogenic therapy in mouse models of colorectal cancer (10).

The urokinase plasminogen activator (uPA) system has been implicated in angiogenesis, growth factor activation, mobilization, ECM remodeling, invasion and metastasis in tumors (11,12). It is currently believed that the expression and activation of uPA play an important role in tumorigenicity, and high endogenous levels of uPA are associated with advanced metastatic cancers (13,14). Therefore, uPA is increasingly being recognized as a candidate target for gene therapy in cancers (15-20).

The purpose of the present study was to examine the effect of rNAPc2 treatment on the invasive ability of NSCLC cells. In the present study, we showed that rNAPc2 inhibited cell invasion and uPA protein production in NSCLC cells. Its inhibitory effect is possibly dependent on the nuclear factor-κB (NF-κB) activation pathway, indicating its potential use in cancer therapy.

Materials and methods

Materials. Isopropyl 1-thio-β-D-galactopyranoside (IPTG), penicillin and streptomycin were purchased from Sigma-Aldrich (St. Louis, MO, USA). SN50 was purchased from Biomol (Plymouth Meeting, PA, USA). TRIzol, Dulbecco's modified Eagle's medium (DMEM) and fetal bovine serum (FBS) were obtained from Life Technologies (Carlsbad, CA, USA). Rabbit polyclonal NF-κB p65 antibody was purchased from Santa Cruz Biotechnology, Inc. (Dallas, TX, USA). Secondary antibodies for western blotting and immunofluorescence were obtained from Amersham Biosciences Corporation (Piscataway, NJ, USA). Other reagents were obtained from Sigma-Aldrich unless stated otherwise.

Generation of bioactive recombinant Ancylostoma caninum anticoagulant peptide c2. For the expression of high levels of rNAPc2 in *E. coli*, we designed and synthesized 14 oligonucleotides corresponding to the protein sequence of NAPc2 using the theoretically optimized codons in *E. coli* (21). These oligonucleotides cover the full-length sense and antisense NAPc2 gene with a 20-bp overlap. The NAPc2 cDNA was cloned into the pTWIN1, yielding pTWIN1-NAPc2. The NAPc2 cDNA was fused with the genes for the intein and chitin binding domain (CBD), which functions as an affinity tag for expression in *E. coli* and purification of rNAPc2 by pH-dependent cleavage. The plasmid was transformed into *E. coli* ER2566 and was grown in LB media induced with 30 mM IPTG for 3 h. The cell lysate was loaded onto a chitin column and the target protein was collected after triggered splicing with 20 mM Tris-HCl, pH 7.2. The target protein rNAPc2 was sequenced from the N-terminus.

Cell culture. A549 and H1299 cells were purchased from the American Type Culture Collection (ATCC) and were maintained in DMEM supplemented with penicillin (50 U/ml), streptomycin (50 U/ml) and 10% FBS.

Cell invasion assay. A Transwell cell culture chamber (Merck Millipore, Bedford, MA, USA) was coated with Matrigel, dried and reconstituted at 37˚C with culture medium. rNAPc2 (0, 3, 6 and 12 μg/ml) was added into the upper chamber. We placed culture medium containing 20% FBS in the lower chamber (24-well plates). Then the cells at $1x10^5$ cells/chamber were added to the upper chamber in DMEM containing 10% FBS. After a 24-h incubation at 37˚C, the suspended media in the lower chamber were removed. The cells that had invaded to the lower side of the filter were fixed in 4% paraformaldehyde and stained with Giemsa solution. The number of cells that passed through the pores into the lower chamber were counted under a phase-contrast microscope. The invasion index is expressed as the ratio of the percent invasion of test cells over the percent invasion of the control cells.

Immunofluorescence. The cells were washed with phosphate-buffered saline (PBS) twice and immediately fixed with 4% paraformaldehyde at 4˚C for 20 min. The cells were incubated with 3% BSA for 30 min and then with the primary antibody against NF-κB p65 overnight at 4˚C followed by incubation with the fluorescence-conjugated secondary antibodies for 1 h at room temperature.

Preparation of cytoplasmic and nuclear extracts. Cytoplasmic and nuclear extracts were prepared according to the instructions of the Nuclear Extract kit from Active Motif (Carlsbad, CA, USA). Briefly, the cells were scraped, washed with phosphate-buffered saline (pH 7.4), resuspended in hypotonic buffer (10 mM HEPES, 1.5 mM $MgCl_2$, 10 mM KCl, 0.2 mM phenylmethylsulfonyl fluoride and 0.5 mM dithiothreitol) and allowed to swell on ice for 10 min. The cells were homogenized in a Dounce homogenizer. The nuclei were separated by spinning at 3,300 x g for 5 min at 4˚C. The supernatant was used as the cytoplasmic extract. The nuclear pellet was extracted in nuclear extraction buffer [20 mM HEPES (pH 7.9), 0.4 M NaCl, 1.5 mM $MgCl_2$, 0.2 mM EDTA, 25% glycerol, 0.5 mM phenylmethylsulfonyl fluoride and 0.5 mM dithiothreitol (DTT)] for 30 min on ice and centrifuged at 12,000 x g for 30 min. The supernatant was used as the nuclear extract. The protein concentrations in the supernatants of both the nuclear and cytoplasmic extracts were measured by the Bio-Rad protein assay. The nuclear and cytoplasmic extracts (30 μg) were resolved by SDS-PAGE, and the levels of phosphorylated IκBα were detected by western blot analysis.

NF-κB transcription factor assay. NF-κB transcription factor assay was performed according to the instructions of the TransAM NF-κB Family Transcription Factor Assay kit from Active Motif.

Total RNA extraction and real-time PCR analysis. Total cellular RNA was isolated using a single step method with TRIzol (Invitrogen, Carlsbad, CA, USA) according to the manufacturer's instructions. Real-time PCR was performed in a final volume of 20 μl containing 3 μl of cDNA sample, 20 pmol of each primer and 2X IQ™ SYBR®-Green Supermix (Bio-Rad Laboratories, Inc., Hercules, CA, USA). The following oligonucleotide primers were used: uPA-FP, 5'-CAG GGCATCTCCTGTGCATG-3'; uPA-RP, 5'-AGCCCTGCCC

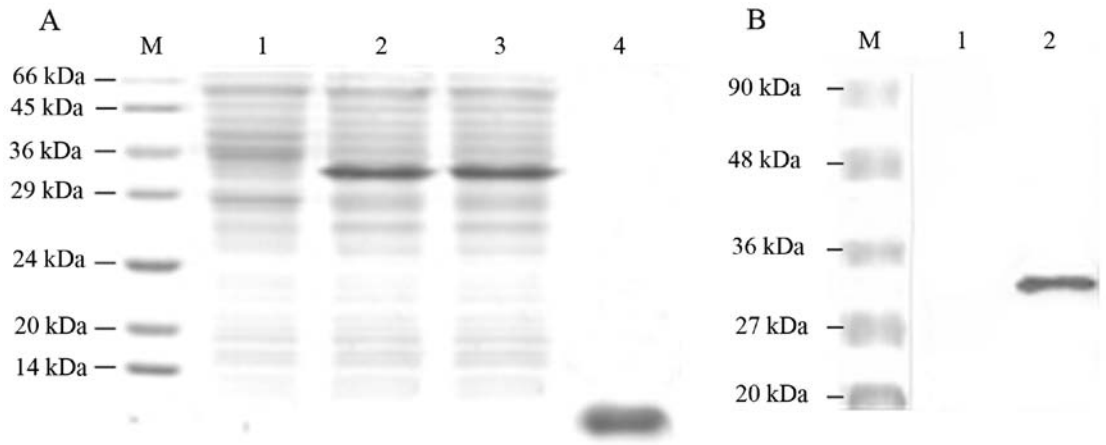

Figure 1. Expression, purification and identification of rNAPc2. (A) Analysis of rNAPc2 by SDS-PAGE. ER2566 cells transformed with the pTWIN1-NAPc2 plasmid were grown in LB media at 37˚C and induced with 30 mM IPTG for expression of the rNAPc2-intein-CBD fusion protein. Lane 1, uninduced ER2566-pTWIN1-NAPc2 lysate; lane 2, IPTG-induced ER2566 pTWIN1-NAPc2 lysate; lane 3, supernatant of IPTG-induced ER2566 pTWIN1-NAPc2 lysate; lane 4, purified rNAPc2; lane M, protein molecular weight standards. (B) Analysis of rNAPc2 by western blotting. The protein with a molecular weight of 34 kDa was detected by the antibody against the CBD. Lane 1, uninduced ER2566 cells; lane 2, IPTG-induced ER2566 cells.

TGAAGTCGTTA-3'; human GAPDH-FP, 5'-ACATGTTCC AATATGATTCCA-3'; human GAPDH-RP, 5'-AGCCCTG CCCTGAAGTCGTTA-3'. We used a denaturing step at 95˚C for 3 min and 40 cycles of 95˚C for 30 sec, 60˚C for 30 sec and 72˚C for 30 sec. Each reaction was run in duplicate, and fluorescence data were collected at the end of the extension step in every cycle.

uPA ELISA. Cells were treated with various concentrations (0, 3, 6 and 12 μg/ml) of rNAPc2 for 24 h. Levels of uPA in the conditioned medium were measured using commercially available uPA ELISA kits (American Diagnostica, Greenwich, CT, USA) according to the manufacturer's instructions.

Chromatin immunoprecipitation (ChIP). An ChIP assay was performed according to the instructions of the ChIP Assay kit from Active Motif. Sequences of promoter-specific primers 5'-GAG GGG GCG GAA GGG GAG AA-3' and 5'-TGT GGT CAG TTT TGT TTG GAT TTG-3' were used to amplify the region of the uPA promoter containing the NF-κB element.

Nude mouse xenograft model. All experimental procedures were conducted in accordance with the Principles of Laboratory Animal Care (Law on Animal Experiments in Denmark, publication 1306, November 23, 2007) and were approved by the West China Second University Hospital Animal Care and Use Committee. Female BALB/c nu/nu mice (4-5 weeks of age) were purchased from the Institute of Experimental Animals, Sichuan University (Chengdu, China). A549 or H1299 cells ($1x10^6$) were suspended in 100 μl PBS and injected subcutaneously in the right posterior flank region of the nude mice. After 10 days, when the tumors reached 5-10 mm in diameter, the mice were randomly divided into 3 groups (5 mice/group). Animals received rNAPc2 as daily intravenous injections of 400 μg/kg or PBS, respectively. Tumor dimensions were measured twice every 5 days by a linear caliper. Tumor volume (mm^3) was calculated using the formula: length x $width^2/2$. All the mice were sacrificed humanely on day 35 after implantation and the extirpated tumors were weighed.

Statistical analysis. Continuous variables are expressed as mean ± SD. Statistical differences were performed using t-test or Mann-Whitney U test. The results are the mean ± SD of values obtained from at least 3 separate experiments. All statistical analyses were performed by the software SPSS for Windows (version 13.0). Differences described as significant in the text correspond to $P<0.05$.

Results

Expression, purification and identification of rNAPc2. ER2566 *E. coli* cells transformed with the pTWIN1-NAPc2 plasmid were grown in LB media at 37˚C and induced with 30 mM IPTG for expression of the rNAPc2-intein-CBD fusion protein. Fig. 1A shows that a large amount of rNAPc2 fusion proteins was detected in the supernatant and the cell lysate. As shown in Fig. 1B, western blot analysis revealed that a product with a molecular weight of 34 kDa was detected by the antibody against the CBD. As the C-terminal cleavage of the intein was favored at a pH 7.2, following splicing of the fusion proteins at a pH 7.2, the eluted rNAPc2 reached a concentration of 4 mg/ml with an expected 10-kDa molecular weight (Fig. 1A). The rNAPc2 was identified by N-terminal sequencing (data not shown).

rNAPc2 inhibits cell invasion and tumor growth in vivo. To provide insight into the possible mechanisms underlying the anticancer effect of rNAPc2, we examined whether rNAPc2 impairs NSCLC cell invasion. In the *in vitro* invasion assay, rNAPc2 obviously inhibited the invasive ability of the NSCLC cells in a dose-dependent manner (Fig. 2). At doses of 3, 6 and 12 μg/ml, treatment with rNAPc2 significantly ($P<0.05$) reduced the cell invasion, respectively, compared with the control group.

To further explore the effect of rNAPc2 on tumor growth *in vivo*, we investigated the ability of rNAPc2 to suppress tumor

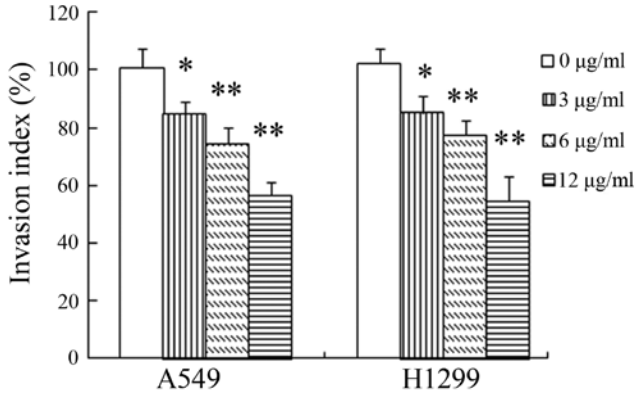

Figure 2. rNAPc2 inhibits NSCLC cell invasion and tumor growth. rNAPc2 obviously inhibited the invasive ability of the NSCLC cells in a dose-dependent manner. rNAPc2 (0, 3, 6 and 12 μg/ml) was added into the upper chamber. The invasion index is expressed as the ratio of the percent invasion of the test cells over the percent invasion of the control cells. *P<0.05; **P<0.01. rNAPc2, nematode anticoagulant protein c2; NSCLC, non-small cell lung cancer.

growth *in vivo* by daily intraperitoneal injection of rNAPc2 at a dose of 400 μg/kg in A549 and H1299 xenograft models in nude mice. rNAPc2 at the dose of 400 μg/kg showed strong inhibition of tumor growth (Fig. 3A). The tumor volume in the mice injected with rNAPc2 was also significantly (P<0.05) smaller than the tumor volume in the mice injected with PBS from day 35 after implantation. The average tumor weight in the mice treated with rNAPc2 on day 35 after the implantation was significantly lower than the tumor weight in the mice treated with PBS alone (Fig. 3B). These results revealed that rNAPc2 significantly inhibited tumor growth in a nude mouse xenograft model.

rNAPc2 reduces cell invasion by inhibiting uPA expression in the NSCLC cells. We hypothesized that rNAPc2 inhibition of NSCLC cell invasion may be due to reduction in the uPA-uPAR system. To test this hypothesis, we investigated uPA and uPAR mRNA expression levels in A549 and H1299 cells following the rNAPc2 treatment. As shown in Fig. 4A and B, rNAPc2 treatment significantly reduced the level of mRNA expression of uPA in cells in a dose-dependent manner but not uPAR. Simultaneously, rNAPc2 reduced uPA protein release in a dose-dependent manner in the supernatants of the A549 and H1299 cells (Fig. 4C). rNAPc2 at 3 μg/ml was sufficient to inhibit uPA protein release in the cell supernatants after rNAPc2 treatment for 24 h (Fig. 4C). Treatment with uPA partially rescued the inhibition of cell invasion by rNAPc2 (P<0.05) (Fig. 4D). These results showed that rNAPc2 reduced cell invasion by inhibiting uPA expression in the NSCLC cells.

rNAPc2 reduces expression and release of uPA by inhibiting NF-κB activation in the NSCLC cell lines. NF-κB is present in

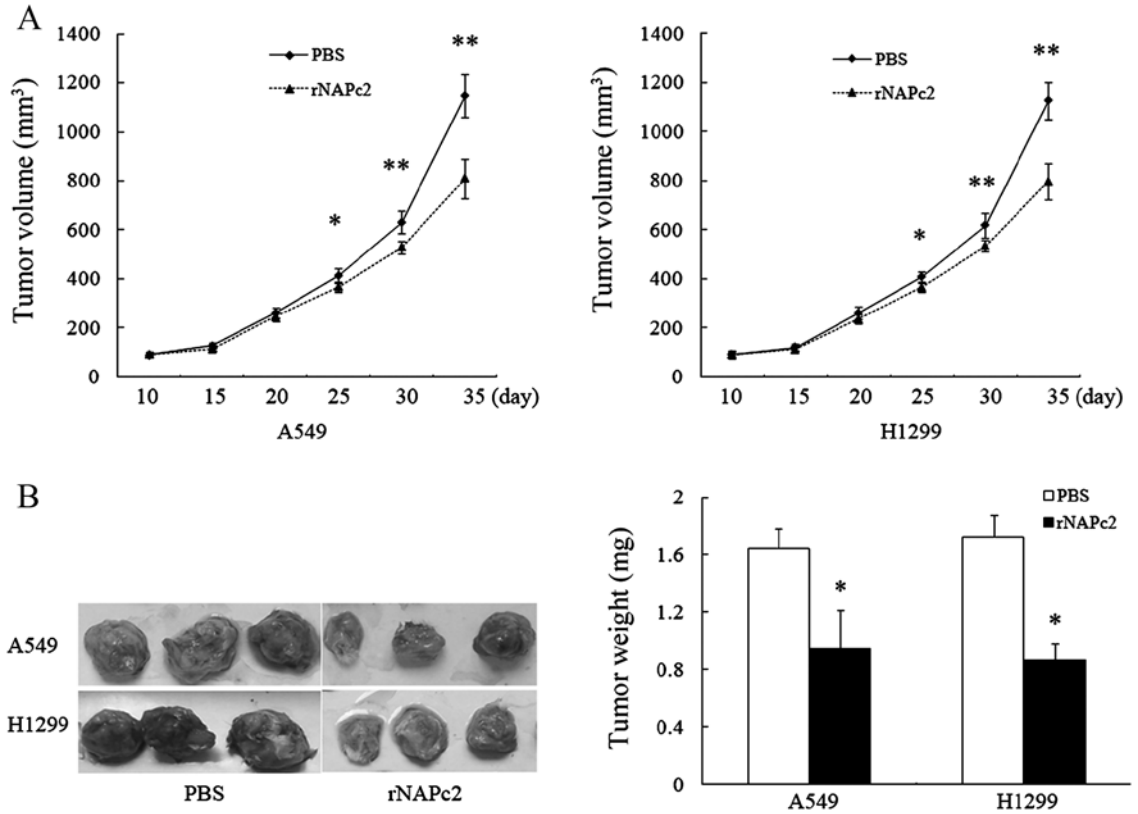

Figure 3. (A) Treatment of rNAPc2 results in a decreased growth rate of the A549 and the H1299 cell tumors in a nude mouse xenograft model. Mice were randomly divided into 2 groups (5 mice/group). Mice received rNAPc2 as a daily intravenous injection of 400 μg/kg or PBS, respectively. The growth of the tumors was observed from 10 to 35 days after implantation. *P<0.05; **P<0.01. (B) Effect of rNAPc2 on tumor growth in a nude mouse xenograft model. All the mice were sacrificed humanely on day 35 after implantation and the extirpated tumors were weighed. The tumor mass in the nude mice treated with rNAPc2 was significantly smaller. *P<0.01. rNAPc2, nematode anticoagulant protein c2; NSCLC, non-small cell lung cancer; PBS, phosphate-buffered saline.

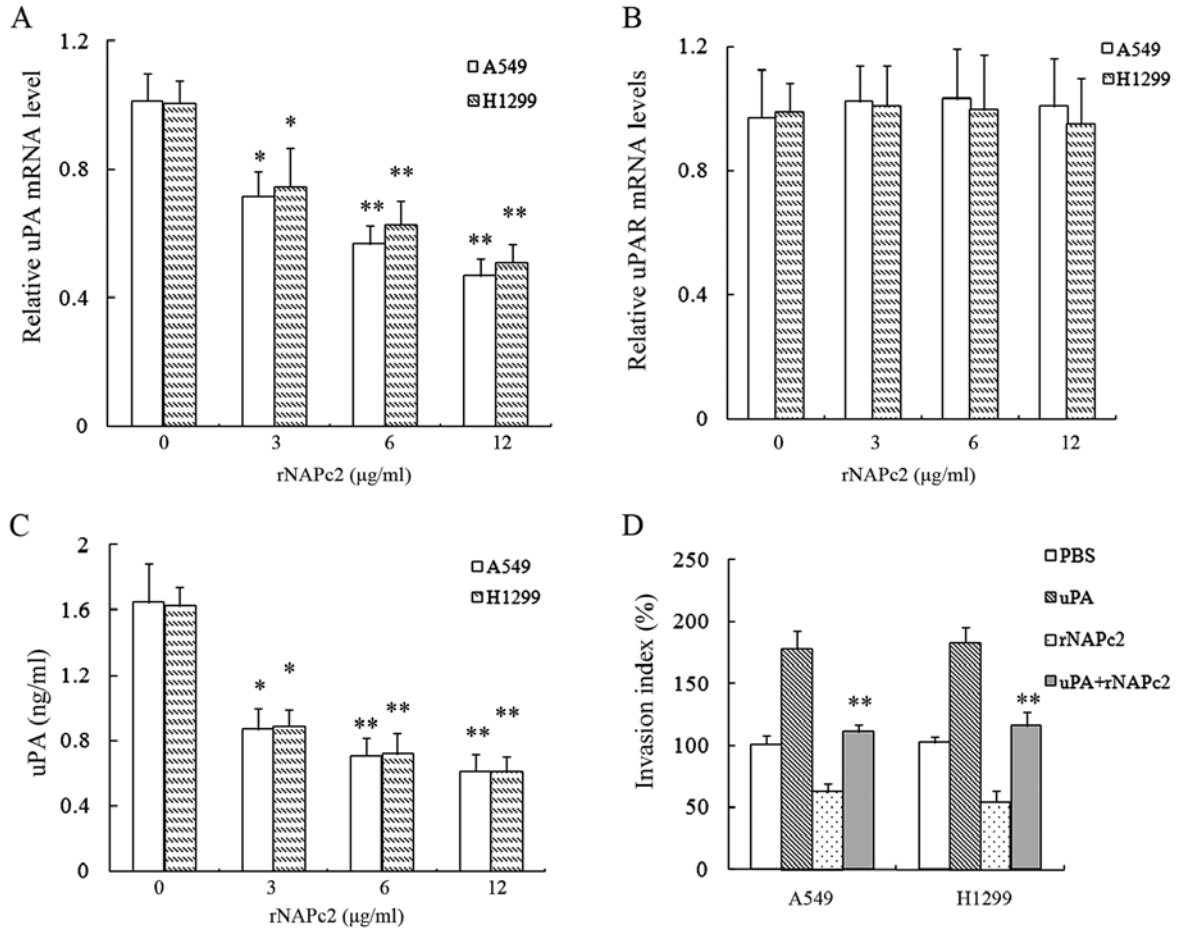

Figure 4. rNAPc2 reduces cell invasion by inhibiting uPA expression in NSCLC cells. (A) rNAPc2 decreased the expression level of uPA mRNA in NSCLC cells in a dose-dependent manner. Cells were treated with various concentrations (0, 3, 6 and 12 μg/ml) of rNAPc2 for 24 h. The relative levels of uPA mRNA were determined by real-time PCR. *P<0.05 and **P<0.01. (B) Effect of rNAPc2 on the expression of uPAR mRNA in the NSCLC cells. The cells were treated with various concentrations (0, 3, 6 and 12 μg/ml) of rNAPc2 for 24 h. The relative level of uPAR mRNA was determined by real-time PCR. The expression level of uPAR mRNA was not significantly different between the rNAPc2 treatment group and the control (P>0.05). (C) rNAPc2 reduces uPA protein release in a dose-dependent manner in the supernatants of the NSCLC cells. The cells were treated with various concentrations (0, 3, 6 and 12 μg/ml) of rNAPc2 for 24 h. The level of uPA in conditioned medium was measured by ELISA. *P<0.05; **P<0.01. (D) Treatment with uPA partially rescued the inhibition of cell invasion by rNAPc2. rNAPc2 (6 μg/ml) was added into the upper chamber after the cells were pre-incubated with the recombinant uPA (100 nmol/l) for 1 h. The cells were allowed to migrate for 24 h at 37˚C. Invasion index was measured. Compared with control, the treatment with the uPA increased the invasion index of the NSCLC cells. *P<0.05 and **P<0.01. rNAPc2, nematode anticoagulant protein c2; NSCLC, non-small cell lung cancer; uPA, urokinase plasminogen activator; NSCLC, non-small cell lung cancer. PBS, phosphate-buffered saline.

the cytoplasm in a resting state and translocates to the nucleus in an activated state. We found that absorbance, which represents the transcriptional activation of NF-κB, was decreased in the rNAPc2-treated cells (Fig. 5A). Incubation with 5 ng/ml TNF-α for 6 h led to nuclear translocation of P65, indicating activation of NF-κB. However, translocation of NF-κB to the nucleus was significantly abolished by rNAPc2 (Fig. 5B).

Phosphorylation and subsequent proteolytic degradation of IκBα liberates NF-κB for nuclear translocation and binding to consensus sequences on promoters and activates NF-κB-regulated genes. We therefore examined cytoplasmic IκBα degradation by western blot analysis. As shown in Fig. 5C, there was notable inhibition in IκBα degradation in the cells following rNAPc2 treatment. We performed an chromatin immunoprecipitation assay to identify that NF-κB can directly bind to the uPA promoter (Fig. 5D).

Then, the level of uPA mRNA expression was analyzed after inhibiting NF-κB activity of the cells. As shown in Fig. 5E, blockage of NF-κB activity reduced the level of uPA mRNA expression in the NSCLC cells. Correspondingly, ELISA analysis revealed that inhibition of NF-κB activity decreased uPA release in the conditioned medium of the NSCLC cells.

Discussion

Cancer patients are highly susceptible to thrombosis, which accounts for a significant portion of the morbidity and mortality of the disease. Antithrombotic drugs including warfarin and low-molecular-weight heparin have been used to prevent deep vein thrombosis and pulmonary embolism in cancer patients (22,23). In addition to preventing venous thromboembolism, antithrombotic therapy inhibits experimental metastasis and prolongs survival in patients with solid tumor malignancies (22). NAPc2 was initially identified as a specific inhibitor of the tissue factor (TF)/factor VIIa complex with novel antithrombotic activity (8). Previous studies have shown that NAPc2 can block angiogenesis, tumor growth and

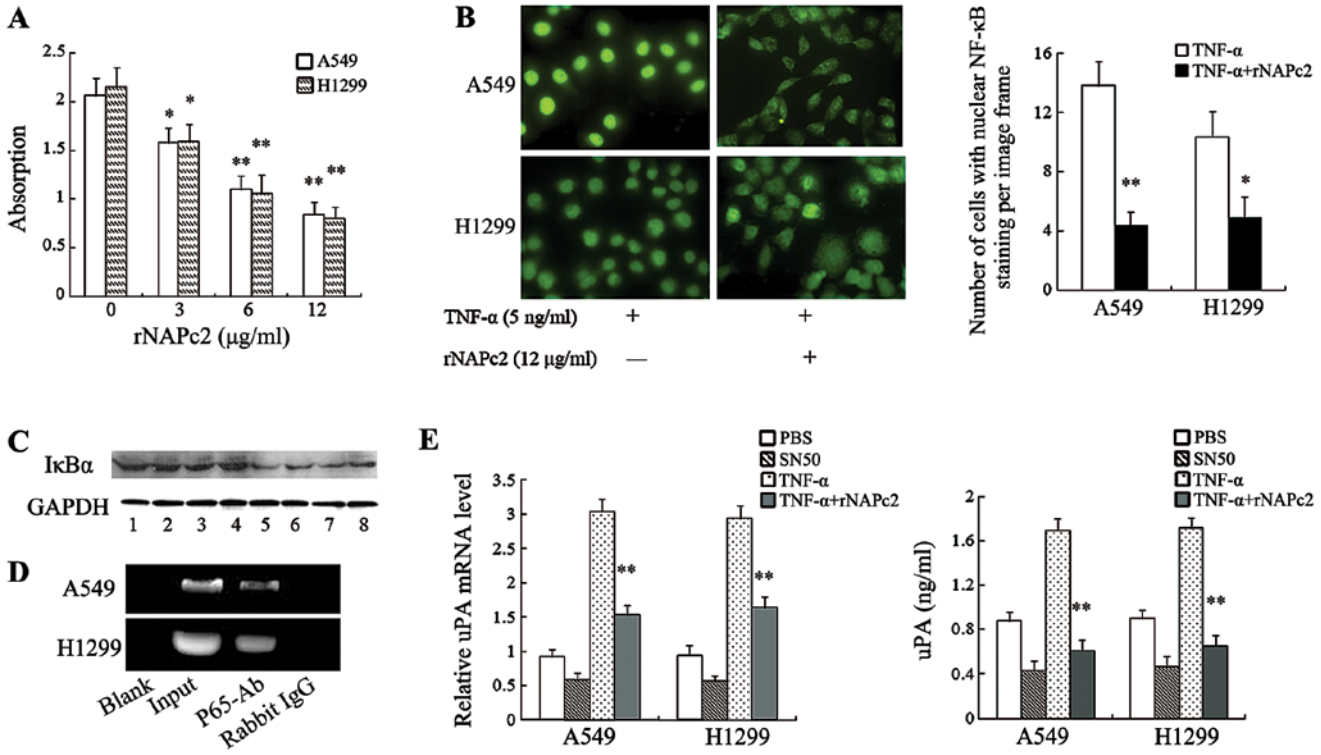

Figure 5. rNAPc2 reduces expression and release of uPA by inhibiting NF-κB activation in NSCLC cells. (A) rNAPc2 inhibited TNF-α-induced NF-κB activation of NSCLC cells as determined by ELISA. Cells were treated with 5 ng/ml TNF-α after pre-incubation with various concentrations (0, 3, 6 and 12 μg/ml) of rNAPc2 for 1 h. After TNF-α treatment for 6 h, NF-κB transcription factor assay of nuclear extracts was performed. NF-κB activation was decreased by rNAPc2. *P<0.05 and **P<0.01. (B) rNAPc2 significantly abolished the translocation of NF-κB to the nucleus induced by TNF-α (magnification, x400). Cells were treated with 5 ng/ml TNF-α after pre-incubation with rNAPc2 (12 μg/ml) for 1 h. After TNF-α treatment for 6 h, translocation of P65 to the nucleus was measured by immunofluorescence. The number of cells with nuclear NF-κB staining was quantified by per image frame. *P<0.05 and **P<0.01. (C) rNAPc2 decreased the IκBα degradation in the NSCLC cell lines. Cytoplasmic IκBα degradation was examined by western blot analysis. Lane 1 (A549) and lane 2 (H1299), controls; lane 3 (A549) and lane 4 (H1299), treated with 3 μg/ml rNAPc2; lane 5 (A549) and lane 6 (H1299), treated with 6 μg/ml rNAPc2; lane 7 (A549) and lane 8 (H1299), treated with 12 μg/ml rNAPc2. Equal protein loading was confirmed using the GAPDH antibody. (D) NF-κB binds to the uPA promoter in the A549 and H1299 cells. ChIP assays were performed to identify uPA promoter sequences containing the putative NF-κB binding sites from chromatin complexes before (input) or after immunoprecipitation (anti-p65 or IgG control). (E) Inhibition of NF-κB activation decreased the level of mRNA expression and release of uPA in conditioned medium from A549 and H1299 cells. Cells were treated with TNF-α (5 ng/ml) after pre-incubation with SN50 (100 μmol/l) for 1 h. The relative levels of uPAR mRNA were determined by real-time PCR. Levels of uPA in conditioned medium were measured by ELISA. SN50 reduced the level of mRNA expression and release of uPA. *P<0.05; **P<0.01, compared with the control (0 μg/ml rNAPc2). rNAPc2, nematode anticoagulant protein c2; NSCLC, non-small cell lung cancer; uPA, urokinase plasminogen activator; NF-κB, nuclear factor-κB; NSCLC, non-small cell lung cancer.

metastasis by decreasing TF/FVIIa activity in experimental mouse models of melanoma and colorectal cancer (8). In contrast, rNAP5, a second nematode anticoagulant protein that specifically inhibits fXa, does not exhibit antitumor activity. Since the hemostatic activity of TF/fVIIa is mediated through activation of fXa, these data suggest that proteolytic activity of TF/fVIIa promotes tumor growth and angiogenesis through an independent novel mechanism (9). In the present study, we employed a novel system to generate high-purity native NAPc2 in high yield by synthesizing the gene for NAPc2 with overlapping oligonucleotides and the IMPACT-TWIN system in *E. coli*. In fact, the generation of native rNAPc2 by traditional expression and purification systems has been difficult. Expression of recombinant protein in *E. coli* usually contains a permanent methionine or another tag that interferes with the bioactivity of the recombinant molecules. Expression of the recombinant protein in yeast and other eukaryotic cells commonly results in a low yield of products. The IMPACT™-TWIN protein fusion and purification system utilizes the inducible self-cleavage activity of engineered protein splicing elements for protein purification and manipulation. The gene for rNAPc22 was fused with the genes for the intein and CBD, allowing us to purify the expressed rNAPc2 with a chitin column and pH-dependent cleavage.

Therefore, we obtained a high yield of rNAPc2 and observed that rNAPc2 obviously inhibited the invasive ability of A549 and H1299 cells in a dose-dependent manner and impaired tumor growth in a xenograft model of nude mice. Recent studies have demonstrated that patients with lung cancer express high levels of the uPA/uPAR system (13). The uPA/uPAR system induces cancer cell proliferation and migration. Inhibition of the uPA/uPAR system function with specific inhibitors significantly decreases cancer invasion and metastasis (24). In fact, plasma levels of uPA were elevated in patients with bladder carcinoma and were associated with features of biologically aggressive disease (14). We showed that rNAPc2 downregulates the expression of uPA mRNA and decreases uPA release.

Several transcription factors, such as NF-κB have been implicated in the regulation of expression of uPA and uPAR (25). NF-κB plays an important role in carcinogenesis. NF-κB induces the expression of diverse target genes

that promote cell proliferation, regulate apoptosis, facilitate angiogenesis and stimulate invasion and metastasis (26,27). Furthermore, many cancer cells show aberrant or constitutive NF-κB activation which mediates resistance to chemotherapy and radiotherapy (28,29). To study the mechanisms responsible for the observed low uPA release and expression in NSCLC cells after rNAPc2 treatment, we detected possible alterations of NF-κB activity. NF-κB is active in the nucleus and is inhibited through its sequestration in the cytoplasm by IκB. IκBs bind to NF-κB dimers and sterically block the function of their nuclear localization sequences, thereby causing their cytoplasmic retention. The NF-κB-IκB complex can also shuttle between the cytoplasm and the nucleus in unstimulated cells (30). We also observed that rNAPc2 caused inhibition of IκBα degradation in the cytoplasm in NSCLC cells. The results showed that activation of NF-κB was significantly abolished by rNAPc2. Furthermore, the results also showed that the blockage of NF-κB activity reduced the level of uPA mRNA expression and cell invasion in the NSCLC cells. Simultaneously, chromatin immunoprecipitation further demonstrated that NF-κB binds to the promoter of uPA. Many signaling pathways activate transcription factors, such as ERK, hypoxia-inducible factor 1α that act on the uPA promoter, driving uPA expression in cancer (31,32). Here, we did not study whether rNAPc2 also modulates these signaling pathways and further research needs to be conducted.

In conclusion, rNAPc2 inhibits cell invasion by inhibiting uPA expression in NSCLC cells. Our results suggest that rNAPc2 may be a potent agent for the prevention of NSCLC progression. Additionally, the results demonstrated that NF-κB plays an important role in NAPc2-induced downregulation of uPA expression.

Acknowledgements

The present study was supported by the National Natural Science Foundation of China (no. 30800633), the Sichuan Province Science and Technology Foundation for Youths (no. 09ZQ026-034), the Sichuan Province Science and Technology Foundation (no. 2012SZ0010), and the Program for Changjiang Scholars and Innovative Research Team in the University (no. IRT 0935).

References

1. Jemal A, Bray F, Center MM, Ferlay J, Ward E and Forman D: Global cancer statistics. CA Cancer J Clin 61: 69-90, 2011.
2. Molina JR, Yang P, Cassivi SD, Schild SE and Adjei AA: Non-small cell lung cancer: Epidemiology, risk factors, treatment, and survivorship. Mayo Clin Proc 83: 584-594, 2008.
3. Schulman S: Advantages and limitations of the new anticoagulants. J Intern Med 275: 1-11, 2014.
4. Mungall D: rNAPc2. Nuvelo. Curr Opin Investig Drugs 5: 327-333, 2004.
5. Schulman S: Patient self-management of anticoagulants reduced arterial thromboembolism and adverse effects. ACP J Club 143: 8, 2005.
6. Vlasuk GP, Bradbury A, Lopez-Kinninger L, Colón S, Bergum PW, Maki S and Rote WE: Pharmacokinetics and anticoagulant properties of the factor VIIa-tissue factor inhibitor recombinant Nematode Anticoagulant Protein c2 following subcutaneous administration in man. Dependence on the stoichiometric binding to circulating factor X. Thromb Haemost 90: 803-812, 2003.
7. Lee AY and Vlasuk GP: Recombinant nematode anticoagulant protein c2 and other inhibitors targeting blood coagulation factor VIIa/tissue factor. J Intern Med 254: 313-321, 2003.
8. Moons AH, Peters RJ, Bijsterveld NR, Piek JJ, Prins MH, Vlasuk GP, Rote WE and Büller HR: Recombinant nematode anticoagulant protein c2, an inhibitor of the tissue factor/factor VIIa complex, in patients undergoing elective coronary angioplasty. J Am Coll Cardiol 41: 2147-2153, 2003.
9. Hembrough TA, Swartz GM, Papathanassiu A, Vlasuk GP, Rote WE, Green SJ and Pribluda VS: Tissue factor/factor VIIa inhibitors block angiogenesis and tumor growth through a nonhemostatic mechanism. Cancer Res 63: 2997-3000, 2003.
10. Zhao J, Aguilar G, Palencia S, Newton E and Abo A: rNAPc2 inhibits colorectal cancer in mice through tissue factor. Clin Cancer Res 15: 208-216, 2009.
11. Raghu H, Nalla AK, Gondi CS, Gujrati M, Dinh DH and Rao JS: uPA and uPAR shRNA inhibit angiogenesis via enhanced secretion of SVEGFR1 independent of GM-CSF but dependent on TIMP-1 in endothelial and glioblastoma cells. Mol Oncol 6: 33-47, 2012.
12. Zhang Y, Kenny HA, Swindell EP, Mitra AK, Hankins PL, Ahn RW, Gwin K, Mazar AP, O'Halloran TV and Lengyel E: Urokinase plasminogen activator system-targeted delivery of nanobins as a novel ovarian cancer therapy. Mol Cancer Ther 12: 2628-2639, 2013.
13. Offersen BV, Pfeiffer P, Andreasen P and Overgaard J: Urokinase plasminogen activator and plasminogen activator inhibitor type-1 in nonsmall-cell lung cancer: Relation to prognosis and angiogenesis. Lung Cancer 56: 43-50, 2007.
14. Shariat SF, Monoski MA, Andrews B, Wheeler TM, Lerner SP and Slawin KM: Association of plasma urokinase-type plasminogen activator and its receptor with clinical outcome in patients undergoing radical cystectomy for transitional cell carcinoma of the bladder. Urology 61: 1053-1058, 2003.
15. Nowicki TS, Moscatello AL, Shin E, Schantz S, Tiwari RK and Geliebter J: The urokinase plasminogen activator system in metastatic papillary thyroid carcinoma: A potential therapeutic target. J Clin Endocrinol Metab 96: 3062-3064, 2011.
16. Kenny HA, Leonhardt P, Ladanyi A, Yamada SD, Montag A, Im HK, Jagadeeswaran S, Shaw DE, Mazar AP and Lengyel E: Targeting the urokinase plasminogen activator receptor inhibits ovarian cancer metastasis. Clin Cancer Res 17: 459-471, 2011.
17. Zhou H, Tang Y, Liang X, Yang X, Yang J, Zhu G, Zheng M and Zhang C: RNAi targeting urokinase-type plasminogen activator receptor inhibits metastasis and progression of oral squamous cell carcinoma in vivo. Int J Cancer 125: 453-462, 2009.
18. Gondi CS, Lakka SS, Dinh DH, Olivero WC, Gujrati M and Rao JS: Intraperitoneal injection of a hairpin RNA-expressing plasmid targeting urokinase-type plasminogen activator (uPA) receptor and uPA retards angiogenesis and inhibits intracranial tumor growth in nude mice. Clin Cancer Res 13: 4051-4060, 2007.
19. Tummalapalli P, Gondi CS, Dinh DH, Gujrati M and Rao JS: RNA interference-mediated targeting of urokinase plasminogen activator receptor and matrix metalloproteinase-9 gene expression in the IOMM-lee malignant meningioma cell line inhibits tumor growth, tumor cell invasion and angiogenesis. Int J Oncol 31: 5-17, 2007.
20. Bauer TW, Liu W, Fan F, *et al*: Targeting of urokinase plasminogen activator receptor in human pancreatic carcinoma cells inhibits c-Met- and insulin-like growth factor-I receptor-mediated migration and invasion and orthotopic tumor growth in mice. Cancer Res 65: 7775-7781, 2005.
21. Hatfield GW and Roth DA: Optimizing scaleup yield for protein production: Computationally Optimized DNA Assembly (CODA) and Translation Engineering. Biotechnol Annu Rev 13: 27-42, 2007.
22. Stevenson JL, Choi SH and Varki A: Differential metastasis inhibition by clinically relevant levels of heparins - correlation with selectin inhibition, not antithrombotic activity. Clin Cancer Res 11: 7003-7011, 2005.
23. Verso M and Agnelli G: New and old anticoagulants in cancer. Thromb Res 129 (Suppl 1): S101-S105, 2012.
24. Nalla AK, Asuthkar S, Bhoopathi P, Gujrati M, Dinh DH and Rao JS: Suppression of uPAR retards radiation-induced invasion and migration mediated by integrin β1/FAK signaling in medulloblastoma. PLoS One 5: e13006, 2010.
25. Moreau M, Mourah S and Dosquet C: β-Catenin and NF-κB cooperate to regulate the uPA/uPAR system in cancer cells. Int J Cancer 128: 1280-1292, 2011.

26. Gyrd-Hansen M and Meier P: IAPs: From caspase inhibitors to modulators of NF-kappaB, inflammation and cancer. Nat Rev Cancer 10: 561-574, 2010.
27. Aurora AB, Biyashev D, Mirochnik Y, Zaichuk TA, Sánchez-Martinez C, Renault MA, Losordo D and Volpert OV: NF-kappaB balances vascular regression and angiogenesis via chromatin remodeling and NFAT displacement. Blood 116: 475-484, 2010.
28. Castro-Gamero AM, Borges KS, da Silva Silveira V, Lira RC, de Paula Gomes Queiroz R, Valera FC, Scrideli CA, Umezawa K and Tone LG: Inhibition of nuclear factor-κB by dehydroxymethylepoxyquinomicin induces schedule-dependent chemosensitivity to anticancer drugs and enhances chemoinduced apoptosis in osteosarcoma cells. Anticancer Drugs 23: 638-650, 2012.
29. Hunter JE, Willmore E, Irving JA, Hostomsky Z, Veuger SJ and Durkacz BW: NF-κB mediates radio-sensitization by the PARP-1 inhibitor, AG-014699. Oncogene 31: 251-264, 2012.
30. Truhlar SM, Torpey JW and Komives EA: Regions of IkappaB alpha that are critical for its inhibition of NF-kappaB.DNA interaction fold upon binding to NF-kappaB. Proc Natl Acad Sci USA 103: 18951-18956, 2006.
31. Tacchini L, Matteucci E, De Ponti C and Desiderio MA: Hepatocyte growth factor signaling regulates transactivation of genes belonging to the plasminogen activation system via hypoxia inducible factor-1. Exp Cell Res 290: 391-401, 2003.
32. Min HJ, Lee Y, Zhao XF, Park YK, Lee MK, Lee JW and Kim S: TMPRSS4 upregulates uPA gene expression through JNK signaling activation to induce cancer cell invasion. Cell Signal 26: 398-408, 2014.